Horizontal Slump of Solid Propellant Motors

L. R. Herrmann* and M. Tamekuni†
Aerojet-General Corporation, Sacramento, Calif.

A stress analysis technique for solid rocket motors stored horizontally is presented. The technique is applicable to motors of finite length with curved or flat ends, consisting of a linear viscoelastic grain bonded to a linear orthotropic elastic thin case. Supporting conditions on the exterior of the shell may be of very general nature (e.g., a line support, strap support, ring support, etc.). The time-dependence of the solution (due to the viscoelastic properties of the grain) is removed by a Laplace transform, and the circumferential spatial dependence due to the transverse gravity loading is treated by a Fourier series. Resulting series of two-dimensional (radial- and axial-dependence) boundary-value problems are solved by the finite-difference technique. The circumferential dependence is then recovered by summing the Fourier series, and the time-dependence is recovered by making use of an approximate Laplace transform inversion technique. Numerical results are given for an example problem in which the end effects are emphasized. Results are contrasted with those given by an approximate solution, neglecting these end effects.

I. Introduction

ONE of the environmental conditions that requires evaluation in assuring the structural integrity of a solid propellant motor is horizontal storage. Only an accurate prediction of the resulting state of stress and deformation in the grain and in the case will allow an appraisal of the effect of such storage on the performance of the rocket.

The determination of the state of stress and strain existing in a cylindrical grain, bonded to a motor case and subjected to a transverse body force, was initially considered by Lianis, Breslau, and Blatz et al.[1–3] These investigations assumed that 1) the shell was rigid and 2) a state of plane strain existed in the grain. The relaxation of the first assumption was considered by Gillis and Valanis.[4, 5] Relaxation of the second assumption was accomplished by Herrmann et al.; however, the solution still does not rigorously apply to cylinders of finite length.[6] It permits evaluation of grains of infinite length subjected to supporting conditions, which varied periodically in the axial direction. Thus, none of the available analyses includes a rigorous treatment of the end effects. In the following section, a technique is presented for the analysis of the horizontal slump of a circular grain of finite length bonded to a flexible elastic case. The grain may have curved or flat ends and the case may be supported in any arbitrary fashion. The motor case is considered to be orthotropic to include motors with filament-wound chambers.

II. Analysis

The analysis of a viscoelastic structure may be reduced to the analysis of a corresponding elastic structure by applying the Laplace transform that removes the time-dependence.[7] Hence, the first step in the analysis of the viscoelastic slump of a rocket motor is the solution of the associated elastic slump problem; in particular, this means the analysis of an isotropic elastic grain bonded to an orthotropic elastic thin motor case and subjected to transverse body forces. The elastic solutions given by Lianis, Breslau, Blatz, Gillis, Valanis, and Herrmann were obtained in closed mathematical form; however, when end effects are included in the analysis, such a solution is not feasible.[1–6] Several investigators have applied finite-difference techniques to the structural analyses of axisymmetric motor configurations subjected to axisymmetric environmental conditions.[8, 9] Because these problems are axisymmetric, it has been necessary only to solve two-dimensional boundary-value problems (governed by two second-order partial differential equations with two dependent and two independent variables). However, the horizontal slump problem results in a three-dimensional boundary-value problem, governed by three second-order partial differential equations with three dependent and three independent variables. In theory, this set of equations can be solved by finite differences, similar to the solution for the axisymmetric problem. However, even with the large capacity of electronic computers, the number of simultaneous linear algebraic equations that can be solved is limited, which in turn limits the number of grid points that can be chosen in the body. Consequently, this restriction precludes the direct finite-difference solution of the three-dimensional elasticity equations at the present time. To circumvent this difficulty, a combination analytical and numerical technique will be applied to the slump problem; the analysis will utilize the solutions of a series of two-dimensional problems that may be solved individually by the finite-difference technique. The reduction of the three-dimensional boundary-value problem to a series of two-dimensional boundary-value problems is accomplished by removing the circumferential dependence through a Fourier series. The solutions of the two-dimensional boundary-value problems define the coefficients in the Fourier series. (This technique has recently been applied to two-dimensional shell problems.[10])

The governing elastic field equations (obtained from the viscoelastic equations by applying the Laplace transform[7]) for the grain are expressed in terms of Papkovich-Neuber displacement functions.[7, 11] The Papkovich-Neuber formulation has the advantage of being accurate for all values of Poisson's ratio and, at the same time, utilizes one less unknown than the displacement formulation given by Herrmann and Toms.[12] The governing elastic field equations expressed in cylindrical coordinates are

$$B_{r,rr} + \frac{1}{r} B_{r,r} - \frac{1}{r^2} B_r + \frac{1}{r^2} B_{r,\theta\theta} + B_{r,zz} - \frac{2}{r^2} B_{\theta,\theta} + \frac{F_r}{\mu} = 0 \quad (1)$$

Presented as Preprint 64-441 at the 1st AIAA Annual Meeting, Washington, D. C., June 29–July 2, 1964; revision received November 20, 1964.

* Senior Research Engineer. Member AIAA.

† Design Engineer.

$$B_{\theta,rr} + \frac{1}{r}B_{\theta,r} - \frac{1}{r^2}B_\theta + \frac{1}{r^2}B_{\theta,\theta\theta} + B_{\theta,zz} + \frac{2}{r^2}B_{r,\theta} + \frac{F_\theta}{\mu} = 0 \quad (2)$$

$$B_{z,rr} + \frac{1}{r}B_{z,r} + \frac{1}{r^2}B_{z,\theta\theta} + B_{z,zz} + \frac{F_z}{\mu} = 0 \quad (3)$$

$$\beta_{,rr} + \frac{1}{r}\beta_{,r} + \frac{1}{r^2}\beta_{,\theta\theta} + \beta_{,zz} - r\frac{F_r}{\mu} - z\frac{F_z}{\mu} = 0 \quad (4)$$

The Papkovich-Neuber displacement functions are denoted by B_r, B_θ, B_z and β.‡ The body forces are written as F_r, F_θ, and F_z. The shear modulus is denoted by μ and partial differentiation is indicated by a comma. The displacements are expressed in terms of the displacement functions by

$$u_r = B_r - \frac{1}{4(1-\nu)}[rB_{r,r} + B_r + zB_{z,r} + \beta_{,r}] \quad (5)$$

$$u_\theta = B_\theta - \frac{1}{4(1-\nu)}\left[B_{r,\theta} + \frac{z}{r}B_{z,\theta} + \frac{1}{r}\beta_{,\theta}\right] \quad (6)$$

$$u_z = B_z - \frac{1}{4(1-\nu)}[rB_{r,z} + B_z + zB_{z,z} + \beta_{,z}] \quad (7)$$

The displacement components are denoted by u_r, u_θ, and u_z, and Poisson's ratio by ν.

The body force components are as follows (Fig. 1):

$$F_r = \rho\cos\theta \qquad F_\theta = -\rho\sin\theta \qquad F_z = 0$$

With these expressions, where ρ is the propellant density, Eq. (4) becomes

$$\beta_{,rr} + \frac{1}{r}\beta_{,r} + \frac{1}{r^2}\beta_{,\theta\theta} + \beta_{,zz} - \frac{r}{\mu}\rho\cos\theta = 0 \quad (8)$$

A particular solution of Eq. (8) is

$$\beta = (\rho/8\mu)r^3\cos\theta \quad (9)$$

For bodies with axisymmetric geometry and loadings that are symmetric about the y axis (Fig. 1), the dependent variables may be expressed in Fourier series as follows:

$$B_r = \sum_{n=0}^{N} A_n(r,z)\cos n\theta \quad (10)$$

$$B_\theta = \sum_{n=1}^{N} B_n(r,z)\sin n\theta \quad (11)$$

$$B_z = \sum_{n=0}^{N} C_n(r,z)\cos n\theta \quad (12)$$

The number of terms included in the series [i.e., the value of N in Eqs. (10–12)] will depend upon the number of terms needed to approximate the circumferential variation of the external supporting forces [e.g., Eq. (33)].

Substitution of Eqs. (9–12) into Eqs. (1–3) yields the following set of governing equations for the Fourier coefficients A_n, B_n, and C_n:

$$A_{n,rr} + \frac{1}{r}A_{n,r} - \frac{1}{r^2}A_n - \frac{n^2}{r^2}A_n + A_{n,zz} - \frac{2n}{r^2}B_n = -\frac{\rho}{\mu}\delta_{1n} \quad (13)$$

$$B_{n,rr} + \frac{1}{r}B_{n,r} - \frac{1}{r^2}B_n - \frac{n^2}{r^2}B_n + B_{n,zz} - \frac{2n}{r^2}A_n = \frac{\rho}{\mu}\delta_{1n} \quad (14)$$

$$C_{n,rr} + \frac{1}{r}C_{n,r} - \frac{n^2}{r^2}C_n + C_{n,zz} = 0 \quad (15)$$

where

$$n = 0, 1, \ldots, N \text{ and } \delta_{1n} = \begin{cases} 0, & n \neq 1 \\ 1, & n = 1 \end{cases}$$

Thus, the three-dimensional equations (1–3) dependent upon r, θ, and z are replaced by a series (a set for each value of n) of two-dimensional equations (13–15) dependent upon r and z. These sets of two-dimensional equations are solved by the finite-difference technique.

Boundary conditions needed for these solutions will now be developed. If displacements and stresses are defined as

$$u_r = \sum_{n=0}^{N} U_n(r,z)\cos n\theta \quad (16)$$

$$u_\theta = \sum_{n=1}^{N} V_n(r,z)\sin n\theta \quad (17)$$

$$u_z = \sum_{n=0}^{N} W_n(r,z)\cos n\theta \quad (18)$$

$$\tau_{rr} = \sum_{n=0}^{N} \sigma_{rn}(r,z)\cos n\theta \quad (19)$$

$$\tau_{zz} = \sum_{n=0}^{N} \sigma_{zn}(r,z)\cos n\theta \quad (20)$$

$$\tau_{rz} = \sum_{n=0}^{N} \sigma_{rzn}(r,z)\cos n\theta \quad (21)$$

$$\tau_{r\theta} = \sum_{n=1}^{N} \sigma_{r\theta n}(r,z)\sin n\theta \quad (22)$$

$$\tau_{\theta z} = \sum_{n=1}^{N} \sigma_{\theta zn}(r,z)\sin n\theta \quad (23)$$

then

$$U_n = A_n - \frac{1}{4(1-\nu)}\left[rA_{n,r} + A_n + zC_{n,r} + \frac{3\rho r^2}{8\mu}\delta_{1n}\right] \quad (24)$$

$$V_n = B_n + \frac{1}{4(1-\nu)}\left[nA_n + \frac{nz}{r}C_n + \frac{\rho r^2}{8\mu}\delta_{1n}\right] \quad (25)$$

$$W_n = C_n - \frac{1}{4(1-\nu)}[rA_{n,z} + C_n + zC_{n,z}] \quad (26)$$

are formed with substitutions from Eqs. (5–7 and 9), and

$$\sigma_{rn} = \frac{\mu}{2(1-\nu)}\left[2(1-\nu)A_{n,r} + 2\nu\left(\frac{nB_n}{r} + \frac{A_n}{r} + C_{n,z}\right) - rA_{n,rr} - zC_{n,rr} - \frac{3\rho r}{4\mu}\delta_{1n}\right] \quad (27)$$

$$\sigma_{zn} = \frac{\mu}{2(1-\nu)}\left[2\nu A_{n,r} + \frac{2n\nu}{r}B_n + \frac{2\nu A_n}{r} + 2(1-\nu)C_{n,z} - rA_{n,zz} - zC_{n,zz}\right] \quad (28)$$

$$\sigma_{rzn} = \frac{\mu}{2(1-\nu)}[(1-2\nu)(C_{n,r} + A_{n,z}) - rA_{n,rz} - zC_{n,rz}] \quad (29)$$

$$\sigma_{r\theta n} = \mu\left[B_{n,r} - \frac{n}{r}A_n - \frac{B_n}{r} - \frac{n}{2(1-\nu)} \times \left(\frac{z}{r^2}C_n - A_{n,r} - \frac{z}{r}C_{n,r} - \frac{\rho r}{4\mu}\delta_{1n}\right)\right] \quad (30)$$

‡ In general β may be chosen as any function that satisfies Eq. (4); the problem then consists of finding the three dependent variables B_r, B_θ, and B_z from Eqs. (1–3).

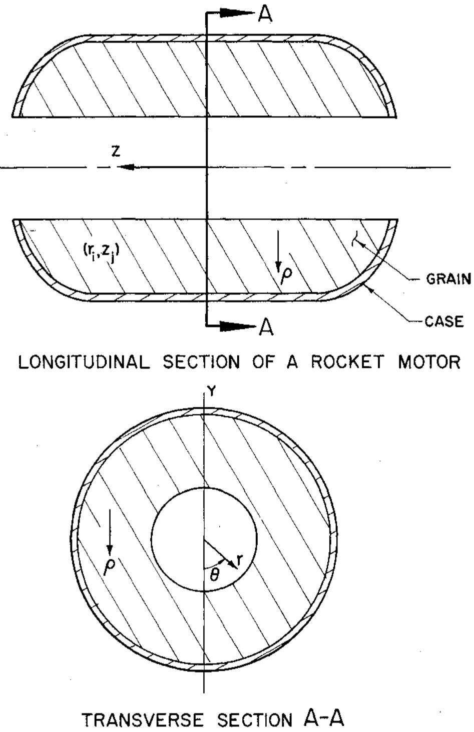

Fig. 1 Rocket motor configuration.

$$\sigma_{\theta z n} = \mu \left\{ B_{n,z} - \frac{n}{2(1-\nu)} \times \left[(1-2\nu)\frac{1}{r} C_n - A_{n,z} - \frac{z}{r} C_{n,z} \right] \right\} \quad (31)$$

are determined by application of Hocke's law and the strain-displacement equations.

By utilizing the preceding expressions, the actual surface conditions may be expressed as boundary conditions for A_n, B_n, and C_n. For example, let one of the prescribed boundary conditions on the surface $r = a$ be

$$\tau_{rz}(a, \theta, z) = f(\theta, z) \quad (32)$$

Then, the function $f(\theta, z)$ is expanded in a Fourier series to yield§:

$$f(\theta, z) = \sum_{n=0}^{N} F_n(z) \cos n\theta \quad (33)$$

Combining Eqs. (32) and (33) with Eqs. (21) and (29), the following boundary conditions for A_n, B_n, and C_n are found:

$$\sigma_{rzn}(a, z) = F_n(z)$$

$$\frac{\mu}{2(1-\nu)} [(1-2\nu)(C_{n,r} + A_{n,z}) - rA_{n,rz} - zC_{n,rz}]|_{r=0} = F_n(z) \quad (34)$$

Thus, Eqs. (13–15), when combined with appropriate boundary conditions, may be solved by the finite-difference technique to yield the values of the unknowns at the grid locations (r_i, z_j) (Fig. 1).

III. Example

As a specific example, the analysis of a motor segment supported by straps will be considered (Fig. 2). The effects of

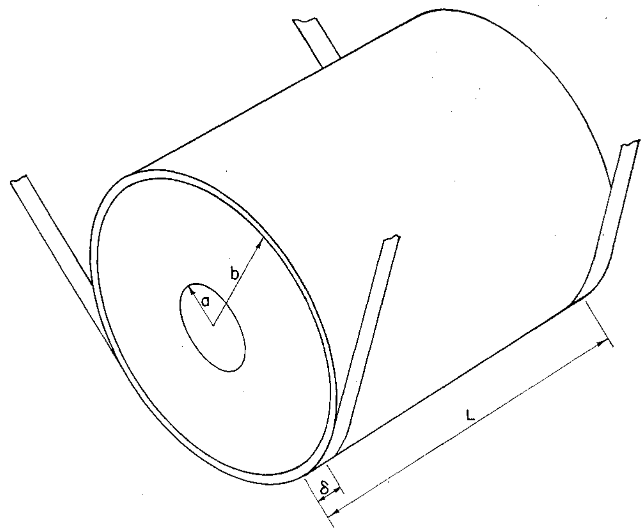

Fig. 2 Motor segment supported by straps.

the straps will be approximated by the supporting pressure shown in Fig. 3 (for the particular problem considered, it was found sufficient to approximate this distribution by the first nine terms of a Fourier cosine series). The surface conditions for this configuration must now be expressed as boundary conditions on the dependent variables A_n, B_n, and C_n. On the surface $r = a$,

$$\tau_{r\theta}(a, \theta, z) = \tau_{rr}(a, \theta, z) = \tau_{rz}(a, \theta, z) = 0 \quad (35)$$

On the surfaces $z = \pm L/2$,

$$\tau_{z\theta}(r, \theta, \pm L/2) = \tau_{zr}(r, \theta, \pm L/2) = \tau_{zz}(r, \theta, \pm L/2) = 0 \quad (36)$$

On the surface $r = b$, the grain is bonded to a thin cylindrical shell; hence, there must be continuity of displacement and stress between the shell and the grain:

$$u_r(b, \theta, z) = -w(\theta, z) \quad (37)$$

$$u_\theta(b, \theta, z) = v(\theta, z) \quad (38)$$

$$u_z(b, \theta, z) = u(\theta, z) \quad (39)$$

$$\tau_{rr}(b, \theta, z) = p^+(\theta, z) \quad (40)$$

$$\tau_{r\theta}(b, \theta, z) = q_\theta^+(\theta, z) \quad (41)$$

$$\tau_{rz}(b, \theta, z) = q_z^+(\theta, z) \quad (42)$$

where u, v, and w are the displacement components of the shell, and p^+, q_θ^+, and q_z^+ are the surface loads applied to the interior of the shell (Fig. 4). The exterior surface loads (q_θ^-, q_z^-, and p^-) applied to the shell are [δ is the strap width and $f(\theta)$ the assumed strap pressure (Figs. 2–4)]

$$q_\theta^-(\theta, z) = 0 \quad (43)$$

$$q_z^-(\theta, z) = 0 \quad (44)$$

$$p^-(\theta, z) = \begin{cases} 0, & (-L/2 + \delta) < z < (L/2 - \delta) \\ f(\theta), & (L/2 - \delta) \le z \le L/2 \\ & \text{and } (-L/2) \le z \le (-L/2 + \delta) \end{cases} \quad (45)$$

Equations (35) and (36), when combined with Eqs. (19–23), yield the following boundary conditions:

$$\sigma_{r\theta n}(a, z) = \sigma_{rn}(a, z) = \sigma_{rzn}(a, z) = 0 \quad (46)$$

$$\sigma_{z\theta n}(r, \pm L/2) = \sigma_{rzn}(r, \pm L/2) = \sigma_{zn}(r, \pm L/2) = 0 \quad (47)$$

Before Eqs. (37–45) are utilized as boundary conditions, the equilibrium of the shell must be considered.

§ The index limit N must be large enough to provide a sufficiently accurate representation of $f(\theta, z)$.

The governing equations for a thin cylindrical shell as given by Timoshenko (the in-plane loading terms and anisotropic effects are given by Flügge¶), where for simplicity only the membrane equations are employed, are[13, 14]:

Equilibrium Equations

$$b(q_z^- - q_z^+) + b\frac{\partial N_z}{\partial z} + \frac{\partial N_{\theta z}}{\partial \theta} = 0 \qquad (48)$$

$$b(q_\theta^- - q_\theta^+) + \frac{\partial N_\theta}{\partial \theta} + b\frac{\partial N_{z\theta}}{\partial z} - Q_\theta = 0 \qquad (49)$$

$$b(p^+ - p^-) + b\frac{\partial Q_z}{\partial z} + \frac{\partial Q_\theta}{\partial \theta} + N_\theta = 0 \qquad (50)$$

Stress Resultant-Displacement Relations (for an orthotropic shell)

$$N_z = h\left[A_{11}\frac{\partial u}{\partial z} + A_{12}\frac{1}{b}\left(\frac{\partial v}{\partial \theta} - w\right)\right] \qquad (51)$$

$$N_\theta = h\left[A_{12}\frac{\partial u}{\partial z} + A_{22}\frac{1}{b}\left(\frac{\partial v}{\partial \theta} - w\right)\right] \qquad (52)$$

$$N_{z\theta} = h\,A_{44}\left(\frac{1}{b}\frac{\partial u}{\partial \theta} + \frac{\partial v}{\partial z}\right) \qquad (53)$$

Combining Eqs. (16–23, 37–45, and 48–53) leads to the following boundary conditions:

$$\frac{nh\,A_{22}}{b^2}U_n - h\,A_{44}V_{n,zz} + \frac{n^2h\,A_{22}V_n}{b^2} + \frac{nh\,(A_{12}+A_{44})}{b}W_{n,z} + \sigma_{r\theta_n}(b,\theta,z) = 0 \qquad (54)$$

$$-h\,A_{11}W_{n,zz} + \frac{n^2h\,A_{44}W_n}{b^2} - \frac{nh}{b}(A_{12}+A_{44})V_{n,z} - \frac{h\,A_{12}}{b}U_{n,z} + \sigma_{rz_n}(b,\theta,z) = 0 \qquad (55)$$

$$\frac{h\,A_{22}}{b^2}U_n + \frac{nh\,A_{22}}{b^2}V_n + \frac{h\,A_{12}}{b}W_{n,z} + \sigma_{r_n}(b,\theta,z) = \begin{cases} 0, \left(-\frac{L}{2}+\delta\right) < z < \left(\frac{L}{2}-\delta\right) \\ F_n, \left(\frac{L}{2}-\delta\right) \le z \le \frac{L}{2} \\ \text{and } \left(-\frac{L}{2}\right) < z < \left(-\frac{L}{2}+\delta\right) \end{cases} \qquad (56)$$

where the Fourier coefficients of $f(\theta)$ are denoted as F_n.

Equations (46, 47, and 54–56), with substitutions from Eqs. (24–31), yield the desired boundary conditions for the dependent variables A_n, B_n, and C_n.** These boundary conditions, in combination with the governing equations (13–15), constitute complete sets of simultaneous equations, which, upon solution by finite-difference technique,[15] provide the values of A_n, B_n, and C_n. The desired stresses and displacements are then found from Eqs. (16–31).[15]

Having thus obtained the solution to the associated elasticity problem, it is necessary to invert it to obtain the viscoelastic solution; however, for realistic grain problems, it is usually impossible to obtain the exact inversion. Therefore, use must be made of an approximate inversion technique. A simple approximate inversion scheme for Laplace transforms was reported by Schapery.[16] The approximate inverse of $\bar{f}(p)$ is

$$f(t) \approx [p\bar{f}(p)]|_{p=1/2t}$$

When the load is applied as a step function of time, the application of this approximate inversion technique simplifies the viscoelastic analysis to one of solving an elasticity problem with time-dependent material properties:

$$\mu(t) \approx \bar{\mu}(p)|_{p=1/2t} \quad \text{and} \quad \nu(t) \approx \bar{\nu}(p)|_{p=1/2t}$$

The Laplace transforms of the viscoelastic material properties are denoted by $\bar{\mu}(p)$ and $\bar{\nu}(p)$.

For extended storage conditions, when the critical state of stress and strain occurs after the material has reached equilibrium, it is sufficient to evaluate the long-time viscoelastic response. This behavior may be readily evaluated by employing the Abel limit theorem.[17] The Abel limit theorem states that, if $f(t)$ is bounded and if the $\lim_{t\to\infty} f(t) = a$ exists, then

$$\lim_{p\to 0} p\,\bar{f}(p) = \lim_{t\to\infty} f(t)$$

Thus, the long-term slump is found by solving the associated elasticity problem with the equilibrium values for the viscoelastic properties.

¶ Notation is illustrated in Fig. 4.

** At the end of the shell, the shell boundary conditions must be employed. They consist of Eq. (56), $N_z = 0$, and $N_{z\theta} = 0$ [Eqs. (51) and (53)].

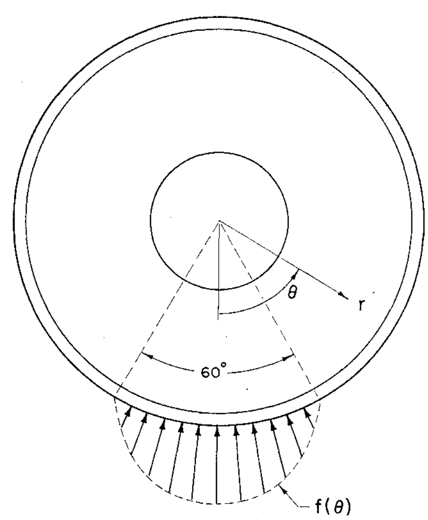

Fig. 3 Assumed strap supporting pressure.

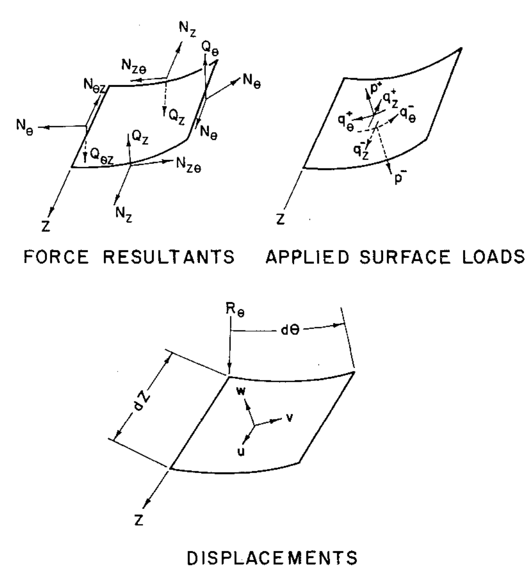

Fig. 4 Shell notation.

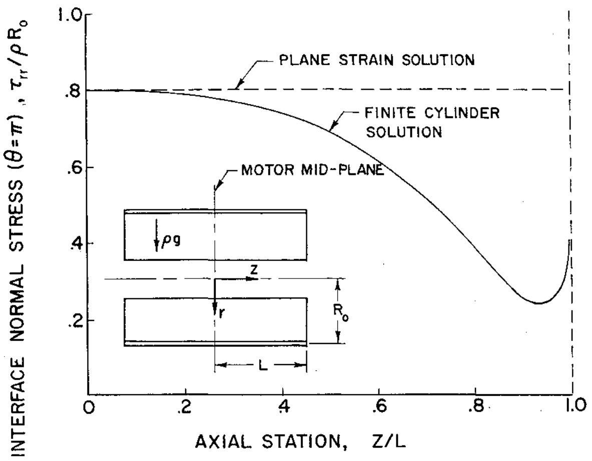

Fig. 5 Plot of normal bond stress.

IV. Numerical Results

In order to illustrate the importance of including the end effects in the analysis of a rocket motor stored horizontally, the numerical solution to a sample problem is given. The particular problem is the analysis of a finite-length rocket grain contained in a rigid case. Approximate solutions to this problem, which neglect end effects (plane strain), were found by Lianis, Breslau, Blatz, et al., and Herrmann et al.; the numerical results obtained are contrasted to those given by Herrmann et al.[1-3, 6] The solution is the long-time viscoelastic response of a typical solid propellant. Figures 5–7 are plots of the bond stresses existing between the grain and the case. The results given in Fig. 5 show that the maximum normal bond stress remains the same (the plane strain results are given by dashed lines); however, Figs. 6 and 7 show that much larger bond shearing stresses exist in the finite-length rocket grain than indicated by the approximate solution. These significant increases in the predicted values of the bond stresses emphasize the necessity of the consideration of these effects.

V. Conclusions

An analysis was developed to determine the state of stress and strain existing in a solid rocket motor stored horizontally. Previous horizontal slump analyses of solid rocket motors were restricted to approximately the motors as infinitely long thick-walled cylinders. These solutions were of closed form. In order to develop an analysis applicable to motors of finite length, it was necessary to employ a numerical solution method. The method employed in this paper permits a realistic representation of the actual motor configuration.

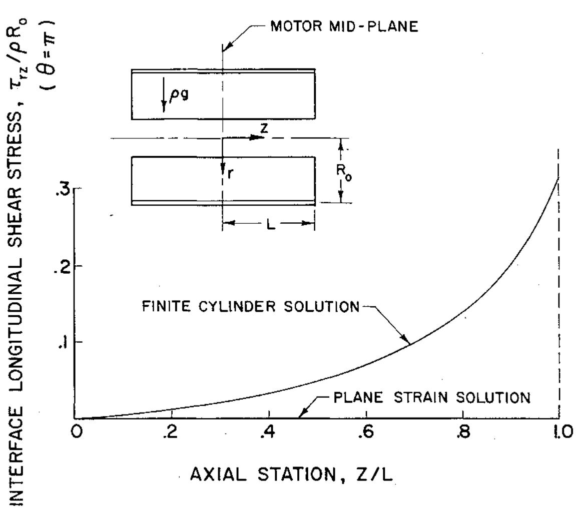

Fig. 6 Plot of longitudinal shear bond stress.

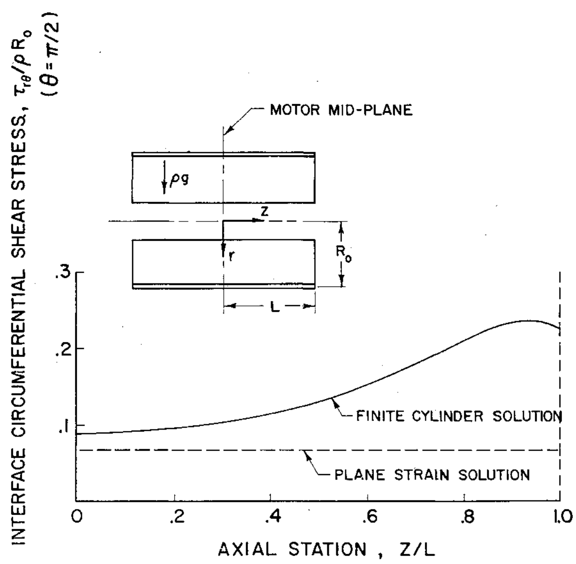

Fig. 7 Plot of circumferential shear bond stress.

References

[1] Lianis, G., "Stresses and strains in solid propellants during storage," ARS J. **32**, 688–692 (1962).

[2] Breslau, D., "Stresses in a gravitating hollow cylinder," Master of Science Thesis, Univ. of California (June 1960).

[3] Blatz, P. J., Ko, W. L., and Zak, A. R., "Fundamental studies relating to the mechanical behavior of solid propellants, rocket grains and rocket motors," Graduate Aeronautical Lab., California Institute of Technology SM62-63, pp. 33–40 (May 1962).

[4] Gillis, G. F., "Elastic stresses and displacements induced in solid propellant rocket motors by transverse gravity forces," Rohm and Haas Co. Rept. P-62-13 (July 1962).

[5] Valanis, K. C. "Horizontal slump of a viscoelastic hollow cylinder contained in a thin elastic shell," Purdue Univ. Rept. A&ES 62-6 (October 1962).

[6] Herrmann, L. R., Tamekuni, M., and Toms, R. M., "New methods for the structural analysis of propellant grains," Bull. Interagency Solid Propulsion Meeting II, 425–446 (July 1963).

[7] Lee, E. H., "Stress analysis in viscoelastic bodies," Quart. Appl. Math. **13**, 183–190 (1955–1956).

[8] Messner, A. M., "Propellant grain stress analysis," *Proceedings of the Seventh JANAF-ARPA-NASA Solid Propellant Group Meeting* (Solid Propellant Information Agency Publications, Silver Spring, Md., 1961), pp. 149–166.

[9] Parr, C. H., "End effects due to shrinkage in propellant grains," *20th Meeting Bulletin of the JANAF-ARPA-NASA Panel on Physical Properties of Solid Propellants* (Solid Propellant Information Agency Publications, Silver Spring, Md., 1961), pp. 71–81.

[10] Budiansky, B. and Radkowski, P. P., "Numerical analyses of unsymmetrical bending of shells of revolution," AIAA J. **1**, 1833–1843 (1963).

[11] Novozhilov, V. V., *Theory of Elasticity* (Israel Program for Scientific Translations, Jerusalem, 1961), pp. 170–172.

[12] Herrmann, L. R. and Toms, R. M., "A reformulation of the elastic field equations, in terms of displacements, valid for all admissible values of Poisson's ratio," J. Appl. Mech. **31**, 140 (March 1964).

[13] Timoshenko, S., *Theory of Plates and Shells* (McGraw-Hill Book Co., Inc., New York, 1940), pp. 389–449.

[14] Flügge, W., *Stresses in Shells* (Springer-Verlag, Berlin, 1962), pp. 19, 293.

[15] Allen, D. N., *Relaxation Methods in Engineering and Science* (McGraw-Hill Book Co., Inc., New York, 1954), pp. 54–125.

[16] Schapery, R. A., "Approximate methods of transform inversion for viscoelastic stress analysis," Graduate Aeronautical Lab., California Institute of Technology SM62-2 (January 1962).

[17] Widder, D. V., *The Laplace Transform* (Princeton University Press, Princeton, N. J., 1946), pp. 185–189.